

光学学报

高分二号全色卫星影像大气校正

郑杨^{1,2}, 李正强^{1,2,3*}, 王思恒^{4**}, 马䶮², 李凯涛^{1,2}, 张玉环⁵, 刘振海⁶, 杨磊库⁷, 侯伟真^{2,3}, 顾浩然^{1,8}, 李殷娜^{2,3}, 姚前^{2,3}, 何卓^{2,3}

¹海南空天信息研究院, 海南 三亚 572032;

²中国科学院空天信息创新研究院, 国家环境保护卫星遥感重点实验室, 北京 100101;

³中国科学院大学, 北京 100049;

⁴中国空间技术研究院遥感卫星总体部, 北京 100094;

⁵生态环境部卫星环境应用中心, 北京 100094;

⁶中国科学院合肥物质科学研究院安徽光学精密机械研究所, 安徽 合肥 230031;

⁷河南理工大学测绘与国土信息工程学院, 河南 焦作 454003;

⁸安徽师范大学地理与旅游学院, 安徽 芜湖 241003

摘要 利用大气辐射传输模型和指数衰减点扩展函数, 发展了一套适用于亚米级分辨率的全色卫星影像的大气校正方法, 该方法充分考虑了大气参数(气溶胶、水汽、臭氧及其他吸收气体等参数)、空间分辨率、背景像元与目标像元的空间距离等对邻近效应的影响。结果表明, 本文建立的大气校正方法能够有效去除大气及周围环境对卫星入瞳信号的影响, 充分解决全色卫星影像中的邻近效应问题, 全面提升了卫星影像的质量(清晰度至少提高了 155%, 对比度至少提高了 115%, 边缘能量至少提高了 247%, 细节能量至少提高了 204%, 调制传递函数至少增大了 169%)。

关键词 大气光学; 全色卫星影像; 高分二号; 大气校正; 邻近效应校正

中图分类号 P407.4; TP79 文献标志码 A

DOI: 10.3788/AOS221549

1 引言

近年来, 随着我国高分辨率对地观测系统重大专项的实施, 越来越多的高分辨率光学卫星载荷进入轨道, 极大地推动了高空间分辨率的全色卫星影像在各领域的业务化应用^[1], 而这些定量化应用在一定程度上都依赖于全色卫星影像大气校正的结果。研究表明: 一方面, 卫星影像在成像过程中会受到大气的干扰, 这部分影响主要源于气溶胶等大气组分对太阳辐射的吸收和散射^[2-5], 大气的散射和吸收效应越强, 大气能见度就越低, 进而使得卫星影像的视觉效果越模糊^[6-8]; 另一方面, 卫星影像在成像过程中也会因目标地物周围环境辐射信息的加入(即邻近效应), 使得影像像元的辐射信息无法真实反映地物信息, 且影像空间分辨率越高, 地物类型越复杂, 邻近效应就越强^[8-10], 从而降低了影像的对比度。因此, 利用大气校正消除大气对卫星载荷入瞳信号的影响、恢复真实地表信息、改善影像质量, 是全色卫星影像定量化遥感应用研究

过程中不可或缺的一环。

传统基于大气辐射传输模型(如 6S 模型、MODTRAN 模型等)的大气校正方法受自身算法限制, 难以准确获取背景像元对目标像元的贡献权重^[4], 因而无法有效解决全色卫星影像的邻近效应问题^[2,4,8]。同时, 全色卫星影像的光谱分辨率较低, 很少被用于分析地物光谱特性, 因而使得目前常用的一些大气校正软件包(如 FLAASH、ATCOR 等)均未开发针对全色影像的大气校正功能, 故发展一套适用于全色卫星影像的大气校正方法迫在眉睫。基于此, 本文以高分二号(GF-2)全色卫星影像为例, 利用大气辐射传输模型和基于指数衰减模型的大气点扩展函数(PSF)^[3], 发展了一套适用于全色卫星影像的大气校正方法。该方法计算简单, 充分考虑了大气组分及周围环境对目标像元卫星入瞳信号的影响, 在保证全色卫星影像信息真实的前提下进一步提高了影像的质量。

调制传递函数(MTF)作为光学卫星成像系统的重要评价指标, 能够全面客观地表征图像的边缘锐利

收稿日期: 2022-07-29; 修回日期: 2022-09-09; 录用日期: 2022-09-21; 网络首发日期: 2022-10-01

基金项目: 海南省重点研发科技合作方向项目(ZDYF2020206)、国家杰出青年科学基金(41925019)、国家自然科学基金(41871269, 41975036)

通信作者: *lizq@radi.ac.cn; **rswangshiheng@163.com

程度和空间细节表达程度^[11],其值的高低能够直接反映成像质量的优劣^[12]。因此,为了综合评价大气校正后全色卫星影像的质量,本文同时采用了传统的图像质量评价指标(清晰度、对比度、边缘能量、细节能量)^[13-16]和MTF指标,全面地评价大气校正结果。

2 方法原理

2.1 全色卫星影像大气校正方法

1) 基于6SV模型的初始大气校正

在对GF-2全色卫星影像进行初始大气校正前,需先借助中国资源卫星应用中心(<http://www.cresda.com/CN/Downloads/dbcs/index.shtml>)下载的PMS2/GF-2传感器的定标系数进行辐射校正,辐射校正公式如下所示:

$$L = K_{\text{Gain}} N_{\text{DN}} + K_{\text{Bias}}, \quad (1)$$

式中: L 为辐射亮度,单位为 $\text{W} \cdot \text{m}^{-2} \cdot \text{sr}^{-1} \cdot \mu\text{m}^{-1}$; N_{DN} 为卫星影像的灰度值,无量纲; K_{Gain} 和 K_{Bias} 为定标系数,单位均为 $\text{W} \cdot \text{m}^{-2} \cdot \text{sr}^{-1} \cdot \mu\text{m}^{-1}$ 。

卫星影像的灰度值经过辐射校正被转换为辐射亮度后,相应的表观反射率 ρ_{TOA} 为

$$\rho_{\text{TOA}} = \frac{\pi L d^2}{E_s \cos \theta_s}, \quad (2)$$

式中: ρ_{TOA} 为表观反射率,无量纲; d 为日地天文单位距离,一般取值为1; E_s 为大气层顶的平均太阳光谱辐照度,单位为 $\text{W} \cdot \text{m}^{-2} \cdot \text{sr}^{-1} \cdot \mu\text{m}^{-1}$; θ_s 为太阳天顶角,单位为°。

输入影像的观测几何、同步大气参数等数据,基于6SV辐射传输模型对表观反射率影像进行初始大气校

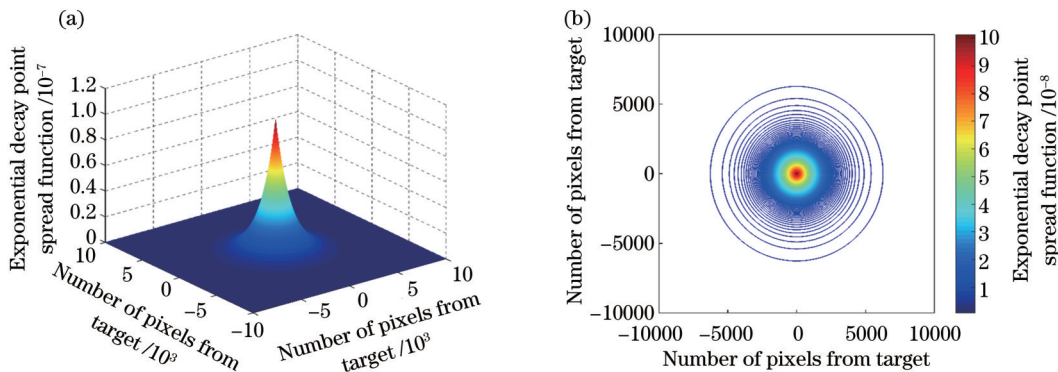


图1 空间分辨率为0.8 m时指数衰减点扩展函数随像元距离的变化。(a)三维曲面图;(b)等值线图

Fig. 1 Exponential decay point spread function varies with pixel distance when spatial resolution is 0.8 m. (a) Three-dimensional surface diagram; (b) contour image

基于6SV模型的初始大气校正是在假设大气水均匀分布、地表为均一朗伯体且处于无云干扰的状态下进行的校正,忽略了背景像元地表类型差异以及邻近效应对目标像元信号的干扰,所以校正后得到的初始地表反射率 ρ_t 是目标像元真实地表反射率与邻近像元空间平均反射率的加权之和:

$$\rho_t = \alpha \rho_s + (1 - \alpha) \rho_e, \quad (4)$$

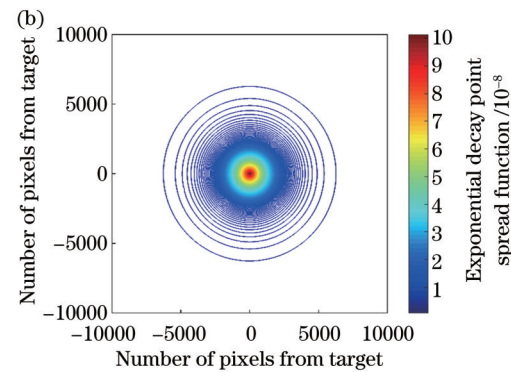
正,得到不考虑地表邻近效应的初始地表反射率 ρ_t ,其辐射传输方程如下所示:

$$\rho_{\text{TOA}} = t_g \left[\rho_a + \frac{T(\theta_s)T(\theta_v)\rho_t}{(1 - \rho_t S)} \right], \quad (3)$$

式中: t_g 为全路径(太阳-地球-卫星)的大气总吸收透过率,无量纲; ρ_a 为程辐射反射率,无量纲; $T(\theta_s)$ 和 $T(\theta_v)$ 分别为向下和向上的辐射透过率,无量纲; S 为半球反照率,无量纲; ρ_t 为初始地表反射率,无量纲; θ_v 为观测天顶角,单位为°。

2) 邻近效应校正

王涛等^[2,4]的研究表明,邻近效应校正的关键在于邻近效应范围及该范围内各像元受邻近效应影响的权重值的确定。邻近效应范围的大小由卫星影像分辨率、大气点扩展函数等因素决定^[3]。本文所采用的GF-2全色卫星影像的空间分辨率为0.8 m,指数衰减点扩展函数值随邻近像元距离的变化如图1所示,可以看出,在目标像元相邻约6250个像元范围(约5 km)内的其他像元均对目标像元的入瞳信号有贡献。在邻近效应校正过程中,为了提高校正精度及速度,一般会选择一个以目标像元为中心、大小为 $(2 \times \delta + 1) \times (2 \times \delta + 1)$ 的窗口进行校正以获取目标像元的背景反射率,其中 δ 为正整数^[2]。研究表明:对于高空间分辨率的卫星影像而言, δ 应大于空间分辨率的7倍^[2,17];当邻近效应的窗口大小达到一定范围后,邻近效应校正窗口的扩大对校正结果的影响极小^[2-3]。因此,综合前人研究^[2-4],本文选用 21×21 大小的窗口对GF-2全色卫星影像进行邻近效应校正。



$$\alpha = \frac{\exp\left(-\frac{\tau}{\cos \theta_v}\right)}{T(\theta_v)}, \quad (5)$$

式中: ρ_s 为目标像元的真实地表反射率; ρ_e 为邻近像元的空间平均反射率; α 为目标像元对最后成像像元的贡献率, $\alpha \in (0, 1)$; τ 为整层大气的光学厚度。邻近像元的空间平均反射率 ρ_e 可由邻近像元的初始地表反

射率与大气点扩展函数的卷积计算近似表示^[18-19]。Vermote等^[20]研究发现,邻近像元对目标像元的贡献随距离的增加呈近似于指数衰减的变化趋势。在许多研究应用中,大气点扩展函数也多采用指数衰减模型^[21-22]。因此,式(4)中 ρ_e 的计算公式可表示为

$$\rho_e(x, y) = \frac{\sum_{j=-n}^n \sum_{i=-n}^n \rho_t(i, j) \times \exp(-r)}{\sum_{j=-n}^n \sum_{i=-n}^n \exp(-r)}, \quad (6)$$

式中: n 为像元坐标; r 为邻近像元到目标像元的实际距离, $r = a \times \sqrt{i^2 + j^2}$, a 为像元空间分辨率,单位为km;(x, y)为目标像元坐标。

虽然能够通过式(6)近似获取邻近像元的空间平均反射率,但和真实邻近像元空间平均反射率相比,结果仍存在误差^[3,10]。因此有必要通过迭代方法预估邻近像元的真实空间平均反射率,消除误差,以获得目标像元的真实地表反射率^[2-3,5]。具体迭代流程如下:

1)首先假设成像区域为均匀朗伯地表,输入观测几何、同步大气参数等数据,基于6SV模型计算不考虑邻近效应的初始地表反射率 $\rho_t^{(0)}$ (即6SV辐射传输方程中的 ρ_t),将其代入基于指数衰减模型的大气点扩展函数[即式(6)],得到邻近像元的零阶真实空间平均反射率 $\rho_e^{(0)}$ 。

$$C_{\text{CLA}} = \frac{1}{m \times n} \sum_{i=1}^m \sum_{j=1}^n \sqrt{\frac{[N_{\text{DN}}(i+1, j) - N_{\text{DN}}(i, j)]^2 + [N_{\text{DN}}(i, j+1) - N_{\text{DN}}(i, j)]^2}{2}}, \quad (9)$$

式中: $N_{\text{DN}}(i, j)$ 为像元灰度值。

2.2.2 对比度

对比度(CON)是指图像的可判别度,可反映图像的清晰度和纹理沟纹的深浅程度,对比度越大,表明图像纹理沟纹越深,视觉效果越清晰^[16]。本文选用了Michelson对比度^[23]来评价全色卫星图像的质量,具体公式如下:

$$C_{\text{CON}} = \frac{\max[N_{\text{DN}}(x, y)] - \min[N_{\text{DN}}(x, y)]}{\max[N_{\text{DN}}(x, y)] + \min[N_{\text{DN}}(x, y)]}. \quad (10)$$

2.2.3 边缘能量

边缘能量(EE,可用 E_{EE} 表示)是图像细节信息的重要组成部分,它具有方向性,利用边缘算子对图像进行卷积处理便可得到图像的边缘能量^[3,16]。 45° 和 135° 两个方向的边缘算子常被用于计算图像边缘 $e(x, y)$,进而得到 E_{EE} 。

$$E_1 = \begin{pmatrix} \frac{1}{6} & -\frac{1}{6} & -\frac{1}{6} \\ -\frac{1}{6} & \frac{4}{6} & -\frac{1}{6} \\ -\frac{1}{6} & -\frac{1}{6} & \frac{1}{6} \end{pmatrix}, E_2 = \begin{pmatrix} -\frac{1}{6} & -\frac{1}{6} & \frac{1}{6} \\ -\frac{1}{6} & \frac{4}{6} & -\frac{1}{6} \\ \frac{1}{6} & -\frac{1}{6} & -\frac{1}{6} \end{pmatrix}, \quad (11)$$

2)根据不考虑邻近效应的目标像元初始地表反射率 ρ_t 是目标像元的真实地表反射率 ρ_s 以贡献率 α 和邻近像元的空间平均反射率 ρ_e 以贡献率 $1 - \alpha$ 混合成像的结果[即式(4)],计算零阶目标像元的真实地表反射率 $\rho_s^{(0)}$ 。

3)进行迭代计算。第 n 阶目标像元的真实地表反射率 $\rho_s^{(n)}$ 可通过第 $n-1$ 阶目标像元的真实地表反射率 $\rho_s^{(n-1)}$ 和第 n 阶邻近像元的真实空间平均反射率 $\rho_e^{(n)}$ 得到:

$$\rho_s^{(n)} = \frac{\rho_s^{(n-1)} - (1 - \alpha)\rho_e^{(n)}}{\alpha}. \quad (7)$$

参考前人研究基础^[2-3,5],上述迭代过程的收敛条件如下:

$$|\rho_s^{(n)} - \rho_s^{(n-1)}| < 0.1. \quad (8)$$

2.2 卫星图像质量评价指标

2.2.1 清晰度

清晰度(CLA)是评价图像边缘信息清晰程度和细节分辨能力的重要指标,可用灰度平均梯度来表征。灰度平均梯度是指图像垂直和水平梯度的变化均值,常用于表征图像清晰度、图像的细节分辨能力和纹理特性,其值越大,表示图像清晰度越高,图像细节越丰富,纹理特征越明显^[15]。CLA可表示为

$$e(x, y) = E_1[N_{\text{DN}}(x, y)] + E_2[N_{\text{DN}}(x, y)], \quad (12)$$

$$E_{\text{EE}} = \frac{1}{(2M+1)^2} \sum_{i=-M}^M \sum_{j=-M}^M e^2(x, y). \quad (13)$$

2.2.4 细节能量

细节能量(DE)是指图像局部区域灰度值方差的均值^[3],反映了图像的细节、纹理等特征的丰富程度,细节能量越大,表明图像的细节信息越丰富,纹理越细致,视觉效果越清晰^[16]。取图像上 $(2M+1) \times (2M+1)$ 的区域,先计算出该区域的灰度值均值 $m(x, y)$ 和方差 $\delta^2(x, y)$,进而得到图像的细节能量 D_{DE} 。

$$m(x, y) = \frac{1}{(2M+1)^2} \sum_{i=-M}^M \sum_{j=-M}^M N_{\text{DN}}(x+i, y+j), \quad (14)$$

$$\delta^2(x, y) = \frac{1}{(2M+1)^2} \sum_{i=-M}^M \sum_{j=-M}^M [N_{\text{DN}}(x+i, y+j) - m(x, y)]^2, \quad (15)$$

$$D_{\text{DE}} = \frac{1}{m \times n} \sum_{i=1}^m \sum_{j=1}^n \delta^2(x, y). \quad (16)$$

2.2.5 MTF

MTF能够定量反映图像质量的敏锐程度,是评价遥感光学系统成像质量和性能的重要指标^[24]。刃边法

作为目前最常用的MTF获取方法,具有严格的理论基础^[25]。所谓刃边,是指灰度值差异较大的两块相邻的均匀亮暗地物的边界,且边缘平直,像刀刃一样^[26]。刃边法通过对刀刃边缘进行采样与拟合得到边缘扩展函数(ESF),对其求导后得到线扩展函数(LSF),最后经傅里叶变换和归一化处理即可得到MTF。奈奎斯特频率为0.5处对应的MTF归一化值即为图像的MTF值。

3 数据介绍

为了充分论证本文所提出的大气校正方法的精确度和适应性,本文以包头定标场的GF-2全色波段卫星

影像(空间分辨率为0.8 m)为例,选取2021年5月29日[大气清洁 $D_{550\text{nm}} = 0.1922$,其中 $D_{550\text{nm}}$ 表示550 nm波段气溶胶光学厚度(AOD)]和2021年8月29日(大气污染 $D_{550\text{nm}} = 0.6689$)两天的数据对其进行大气校正。表1列举了相对应的大气和观测几何参数,其中大气模式中的水汽和臭氧数据、气溶胶模型参数,以及气溶胶光学厚度均来自接近卫星影像过境时间的AERONET地基观测数据(<https://aeronet.gsfc.nasa.gov/>)。通过分析Moderate Resolution Imaging Spectroradiometer (MODIS)和AERONET的气溶胶光学厚度数据(表2),得到与GF-2卫星过境时空近乎同步的550 nm波段的气溶胶光学厚度值(表1)。

表1 GF-2全色波段影像大气和观测几何参数(450~900 nm)

Table 1 Atmospheric parameters and observed geometric parameters of GF-2 panchromatic band image (450~900 nm)

| Imaging time | 2021-05-29T11:34:52 | 2021-08-16T11:34:01 |
|---|-----------------------------|-----------------------------|
| Solar zenith angle / (°) | 23.4457 | 31.3780 |
| Solar azimuth angle / (°) | 139.899 | 145.050 |
| Satellite zenith angle / (°) | 3.4875 | 3.4877 |
| Satellite azimuth angle / (°) | 96.2494 | 285.9640 |
| Aerosol model | Sun-photometer measurements | Sun-photometer measurements |
| $D_{550\text{nm}}$ | 0.1922 | 0.6689 |
| Water vapor content / ($\text{g}\cdot\text{cm}^{-2}$) | 0.8092 | 1.7115 |
| Ozone content / ($\text{g}\cdot\text{cm}^{-2}$) | 7.1709×10^{-4} | 6.3409×10^{-4} |

表2 Terra MODIS产品和AERONET包头地基观测站点获得的气溶胶光学厚度

Table 2 AOD of Terra MODIS product and AOD measured at AERONET Baotou site

| Imaging time | 2021-05-29T11:34:52 | 2021-08-16T11:34:01 |
|---|---------------------|---------------------|
| $D_{550\text{nm}}$ of AERONET Baotou site | 0.1922 | 0.6689 |
| $D_{550\text{nm}}$ of MODIS | 0.128 | 0.653 |

4 分析与讨论

利用本文所提出的针对全色卫星影像的大气校正方法,对包头定标场在清洁和污染两种天气情况下的GF-2全色卫星影像进行大气校正,结果如图2所示,各影像的质量评价参数对比结果如图3和图4所示。为了定量对比分析大气校正前后各影像的质量评价参数结果,本文将图3和图4中各质量评价参数的对比结果汇总到表3中。

对比图2(a)、(c)以及图2(d)、(f)可以看出:无论是污染还是清洁的大气状况,校正后的全色卫星影像在视觉效果上均得到提升,地物轮廓变得清晰,纹理信息更为丰富,地物辨识度也得到了显著提高。对比图2(a)、(b)以及图2(d)、(e)可以看出:对于高分辨率的全色卫星影像而言,忽略邻近效应的大气校正方法仅实现了影像亮度的提升,对影像清晰度的提升并不明显,尤其是在大气污染的情况下,校正后的影像地物边缘仍较为模糊,不利于影像的目视解译和地物轮廓的提取,进而证明了邻近效应校正对高分辨率的全色卫

星影像而言必不可少。

对比图3中校正前后各影像的质量评价参数,可以直观地看出:虽然不考虑邻近效应的大气校正方法能够提升全色卫星影像的清晰度、对比度、边缘能量和细节能量,但提升能力有限,尤其是在大气污染(低大气能见度)的情况下。由图2(b)可以看出:校正后的影像地物边缘仍旧模糊,辨识度不高;本文所提出的大气校正方法考虑了邻近效应校正,无论是污染还是清洁的大气状况,校正后的影像的清晰度、对比度、边缘能量和细节能量都实现了成倍的提升,即便是在大气污染(低大气能见度)的情况下,该校正方法也能把影像的质量提高到大气清洁时校正后影像的质量。从图4校正前后各影像的MTF对比图中可以看出:邻近效应校正后的全色卫星影像的MTF得到显著提升,且MTF曲线的变化趋势也更为缓慢,这表明该大气校正方法校正后的全色卫星影像的清晰度更高,地物边缘锐利程度更大,地物轮廓更为清晰,空间细节也更为丰富,影像质量也更好。

从表3中的数据中可知:本文所提出的大气校正

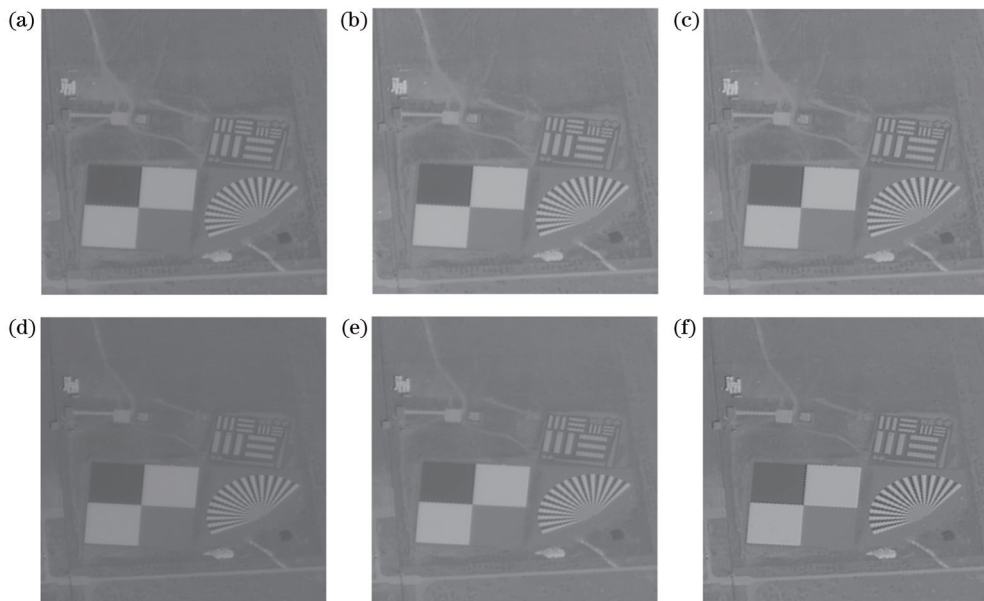


图2 大气校正前后的GF-2全色波段卫星影像。校正前(a)污染大气和(d)清洁大气表观反射率图;大气辐射校正后(b)污染大气和(e)清洁大气初始地表反射率图;邻近效应校正后(c)污染大气和(f)清洁大气真实地表反射率图

Fig. 2 GF-2 panchromatic band satellite images before and after atmospheric correction. Apparent reflectance images of (a) polluted atmosphere and (d) clean atmosphere before atmospheric correction; initial surface reflectance images of (b) polluted atmosphere and (e) clean atmosphere after atmospheric radiation correction; true surface reflectance images of (c) polluted atmosphere and (f) clean atmosphere after adjacency effect correction

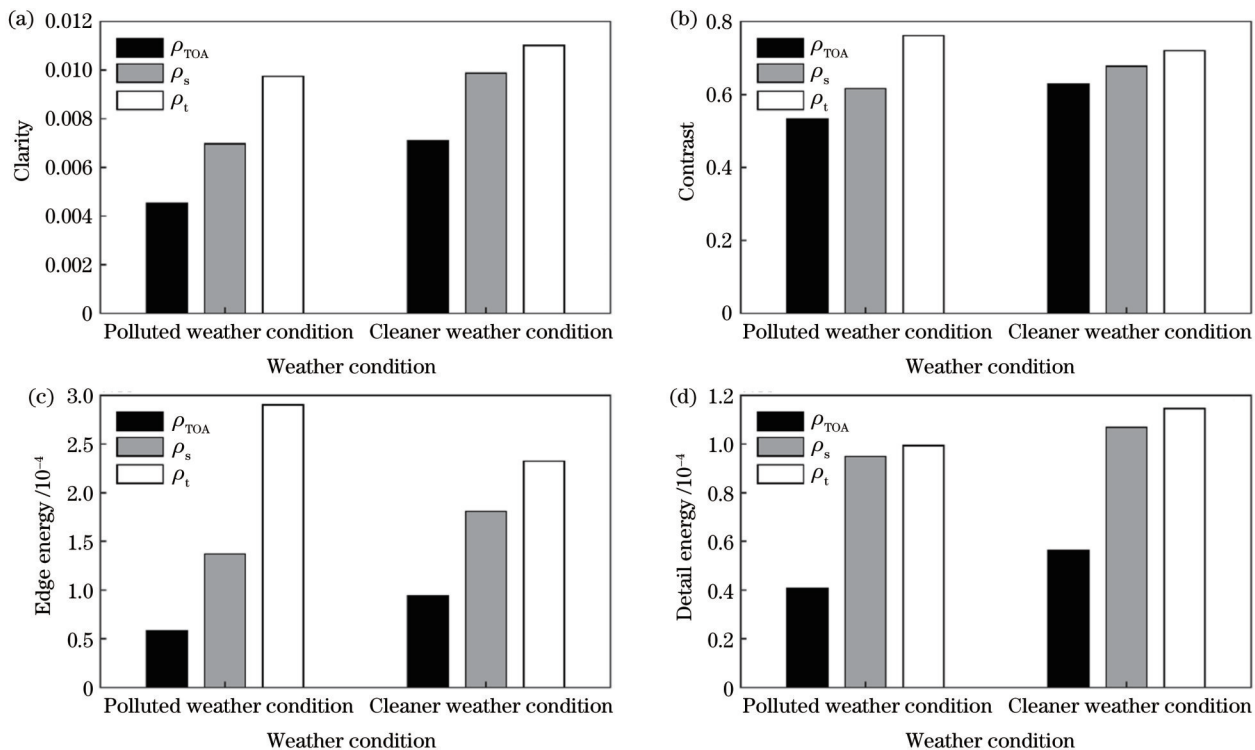


图3 校正前后全色波段卫星影像的清晰度、对比度、边缘能量和细节能量结果对比。(a)清晰度；(b)对比度；(c)边缘能量；(d)细节能量

Fig. 3 Comparison of clarity, contrast, edge energy, and detail energy of panchromatic band satellite images before and after atmospheric correction. (a) Clarity; (b) contrast; (c) edge energy; (d) detail energy

方法校正得到的地表反射率图像的清晰度相较于表观反射率图像至少提高了 155%，对比度至少提高了 247%，边缘能量至少提高了 247%，细节能量至少提高了 204%，MTF 至少提高了 169%。以上评价参数

的对比结果表明本文所提出的针对全色卫星影像的大气校正方法在清洁和污染的大气状况下,都能够有效去除成像过程中大气及周围环境对卫星载荷入瞳信号

的影响,恢复影像真实地表信息,提高影像清晰度,增强影像对比度,使得影像中的地物信息的空间细节更为丰富。

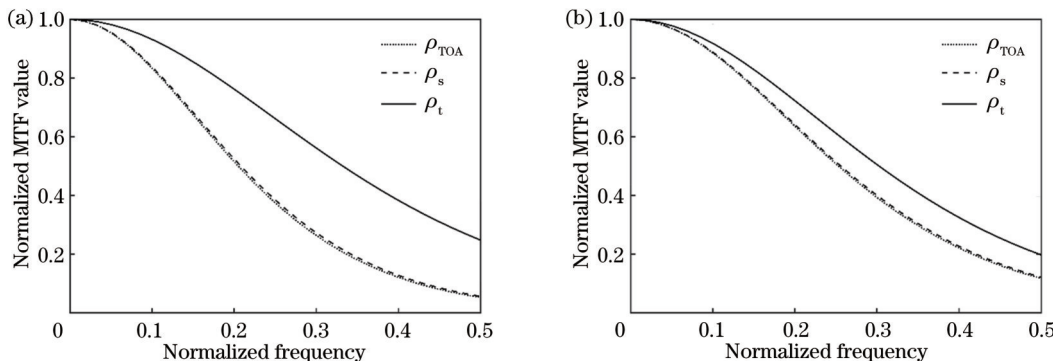


图4 校正前后全色波段卫星影像的MTF。(a)污染大气;(b)清洁大气

Fig. 4 MTF of panchromatic band satellite images before and after atmospheric correction. (a) Polluted atmosphere; (b) clean atmosphere

表3 大气校正对全色卫星影像质量改进的量化对比

Table 3 Comparison of quantitative improvement of panchromatic band satellite images by atmospheric correction unit: %

| Weather condition | Clarity improvement | | Contrast improvement | | Edge energy improvement | | Detail energy improvement | | Normalized MTF (normalized frequency is 0.5) | |
|-------------------|---------------------|---------------------|----------------------|---------------------|-------------------------|---------------------|---------------------------|---------------------|---|---------------------|
| | ρ_s/ρ_{TOA} | ρ_t/ρ_{TOA} | ρ_s/ρ_{TOA} | ρ_t/ρ_{TOA} | ρ_s/ρ_{TOA} | ρ_t/ρ_{TOA} | ρ_s/ρ_{TOA} | ρ_t/ρ_{TOA} | ρ_s/ρ_{TOA} | ρ_t/ρ_{TOA} |
| Clean weather | 139 | 155 | 108 | 115 | 192 | 247 | 190 | 204 | 104 | 169 |
| Polluted weather | 154 | 216 | 116 | 143 | 235 | 497 | 234 | 245 | 107 | 474 |

5 结 论

全色卫星影像具有亚米级别的高空间分辨率,易受到大气吸收和散射效应以及邻近效应的影响,使得卫星影像质量下降。因此,在应用全色卫星影像之前,需对其进行大气校正以改善影像质量。而目前常规的大气校正软件均无法对全色卫星影像进行大气校正,故常用数字图像处理的方法来改善全色卫星影像的质量,但数字图像处理方法在提升影像质量的同时往往会带来噪声和过度增强的问题。本文所提出的大气校正方法在6SV辐射传输模型的基础上,结合了基于指数衰减模型的大气点扩展函数,充分考虑了大气参数(气溶胶、水汽、臭氧及其他吸收气体等参数)、空间分辨率、背景像元与目标像元的空间距离等对邻近效应的影响,能够有效去除全色卫星影像成像过程中大气及周围环境对卫星载荷入瞳信号的影响,恢复成像区域因大气影响而被掩盖的地表真实信息,充分改善低大气能见度情况下全色卫星影像的质量。

在对校正后的全色卫星影像质量进行评价后发现,相较于传统的图像质量评价指标,MTF更能体现邻近效应校正对亚米级全色卫星影像质量的改善,进而突出了邻近效应校正在全色卫星影像大气校正中的不可或缺性;同时,MTF曲线的变化趋势、数值的高低

能够更为全面客观地反映图像的空间敏锐程度和图像质量的优劣。因此,在对亚米级卫星影像(如全色卫星影像)进行图像质量评价时,建议将MTF指标纳入图像质量评价体系。

参 考 文 献

- [1] 童旭东.中国高分辨率对地观测系统重大专项建设进展[J].遥感学报,2016,20(5): 775-780.
Tong X D. Development of China high-resolution earth observation system[J]. Journal of Remote Sensing, 2016, 20(5): 775-780.
- [2] 王涛.亚米级空间分辨率光学卫星影像大气辐射校正研究[D].合肥:中国科学技术大学,2021.
Wang T. Research on atmospheric radiation correction of optical satellite imagery with sub-meter spatial resolution[D]. Hefei: University of Science and Technology of China, 2021.
- [3] 马葵.高空间分辨率光学遥感卫星同步大气校正研究[D].北京:中国科学院大学,2016.
Ma Y. Study on synchronous atmospheric correction of high-resolution optical remote sensing satellite[D]. Beijing: University of Chinese Academy of Sciences, 2016.
- [4] 王涛,周楠,易维宁,等.亚米级光学卫星影像邻近效应校正[J].物理学报,2021,70(13): 139101.
Wang T, Zhou N, Yi W N, et al. Adjacency effect correction of optical satellite image with sub-meter spatial resolution[J]. Acta Physica Sinica, 2021, 70(13): 139101.
- [5] Wang T, Du L L, Yi W N, et al. An adaptive atmospheric correction algorithm for the effective adjacency effect correction of submeter-scale spatial resolution optical satellite images:

- application to a WorldView-3 panchromatic image[J]. *Remote Sensing of Environment*, 2021, 259: 112412.
- [6] 王涛, 周川杰, 易维宁, 等. 基于大气校正提升亚米级卫星影像质量[J]. *光学学报*, 2021, 41(11): 1101002.
Wang T, Zhou C J, Yi W N, et al. Improving quality of sub-meter satellite image based on atmospheric correction[J]. *Acta Optica Sinica*, 2021, 41(11): 1101002.
- [7] 姚群力, 胡显, 雷宏. 基于多尺度卷积神经网络的遥感目标检测研究[J]. *光学学报*, 2019, 39(11): 1128002.
Yao Q L, Hu X, Lei H. Object detection in remote sensing images using multiscale convolutional neural networks[J]. *Acta Optica Sinica*, 2019, 39(11): 1128002.
- [8] Kaufman Y J. Effect of the Earth's atmosphere on contrast for zenith observation[J]. *Journal of Geophysical Research*, 1979, 84(C6): 3165-3172.
- [9] Lyapustin A I, Kaufman Y J. Role of adjacency effect in the remote sensing of aerosol[J]. *Journal of Geophysical Research: Atmospheres*, 2001, 106(D11): 11909-11916.
- [10] 汤兴, 易维宁, 杜丽丽, 等. 高分一号卫星多光谱遥感图像邻近效应校正研究[J]. *光学学报*, 2016, 36(2): 0228003.
Tang X, Yi W N, Du L L, et al. Adjacency effect correction study of GF-1 satellite multi-spectral remote sensing images[J]. *Acta Optica Sinica*, 2016, 36(2): 0228003.
- [11] Pagnutti M, Blonski S, Holekamp K, et al. Measurement sets and sites commonly used for high spatial resolution image product characterization[R]. Mississippi: John C. Stennis Space Center, 2006.
- [12] 程结海. 遥感成像系统MTF参数测定的刃边法改进[J]. *河南理工大学学报(自然科学版)*, 2016, 35(4): 507-511.
Cheng J H. The improving the edge method for the MTF measurement of remote sensing imaging system[J]. *Journal of Henan Polytechnic University (Natural Science)*, 2016, 35(4): 507-511.
- [13] 姚烨. 高分辨率视频卫星影像超分辨率重建技术研究[D]. 长春: 中国科学院长春光学精密机械与物理研究所, 2018.
Yao Y. Research on super-resolution reconstruction of high resolution video satellite images[D]. Changchun: Changchun Institute of Optics, Fine Mechanics and Physics, Chinese Academy of Sciences, 2018.
- [14] 徐宁珊. 可见光遥感图像质量评价与像质提升技术研究[D]. 成都: 中国科学院光电技术研究所, 2021.
Xu N S. Research on image quality assessment and improvement for visible remote sensing image[D]. Chengdu: Institute of Optics and Electronics, Chinese Academy of Sciences, 2021.
- [15] 孙百龙. 航天测控光学系统图像质量评价方法研究[D]. 哈尔滨: 哈尔滨工业大学, 2019.
Sun B L. Research on image quality evaluation of optical survey and control system[D]. Harbin: Harbin Institute of Technology, 2019.
- [16] 曾彩云. 国产高分卫星影像质量评价及特征分析[D]. 成都: 成都理工大学, 2017.
- Zeng C Y. The quality assessment and feature analysis of domestic high resolution satellite images[D]. Chengdu: Chengdu University of Technology, 2017.
- [17] Richter R. A fast atmospheric correction algorithm applied to Landsat TM images[J]. *International Journal of Remote Sensing*, 1990, 11(1): 159-166.
- [18] 程春梅, 李渊, 韦玉春, 等. 太湖沿岸水体高分一号影像的邻近效应校正[J]. *激光与光电子学进展*, 2018, 55(10): 102803.
Cheng C M, Li Y, Wei Y C, et al. Correction of the adjacency effect for GF-1 image in coastal waters of Taihu Lake[J]. *Laser & Optoelectronics Progress*, 2018, 55(10): 102803.
- [19] Li Z Q, Xie Y Q, Hou W Z, et al. In-orbit test of the polarized scanning atmospheric corrector (PSAC) onboard Chinese environmental protection and disaster monitoring satellite constellation HJ-2 A/B[J]. *IEEE Transactions on Geoscience and Remote Sensing*, 2022, 60: 4108217.
- [20] Vermote E F, El Saleous N, Justice C O, et al. Atmospheric correction of visible to middle-infrared EOS-MODIS data over land surfaces: background, operational algorithm and validation [J]. *Journal of Geophysical Research: Atmospheres*, 1997, 102(D14): 17131-17141.
- [21] Prieto-Amparán J, Villarreal-Guerrero F, Martínez-Salvador M, et al. Atmospheric and radiometric correction algorithms for the multitemporal assessment of grasslands productivity[J]. *Remote Sensing*, 2018, 10(2): 219.
- [22] 刘成玉, 陈春, 张树清, 等. ETM图像大气邻近效应校正[J]. *光谱学与光谱分析*, 2010, 30(9): 2529-2532.
Liu C Y, Chen C, Zhang S Q, et al. Atmospheric adjacency effect correction of ETM images[J]. *Spectroscopy and Spectral Analysis*, 2010, 30(9): 2529-2532.
- [23] Wang Z, Bovik A C. Mean squared error: love it or leave it? A new look at signal fidelity measures[J]. *IEEE Signal Processing Magazine*, 2009, 26(1): 98-117.
- [24] Leger D, Viallefont F, Hillairet E, et al. In-flight refocusing and MTF assessment of SPOT5 HRG and HRS cameras[J]. *Proceeding of SPIE*, 2003, 4884: 224-231.
- [25] 刘亮, 李显彬, 姜小光, 等. 刃边法的MTF评价精度分析[J]. *中国科学院研究生院学报*, 2012, 29(6): 786-792.
Liu L, Li X B, Jiang X G, et al. Accuracy of knife-edge method in MTF assessment[J]. *Journal of Graduate University of Chinese Academy of Sciences*, 2012, 29(6): 786-792.
- [26] 黄黎. 中低分辨率卫星成像系统的MTF在轨检测方法研究[D]. 南京: 南京理工大学, 2009.
Huang L. Research on MTF in-orbit detection method of medium and low resolution satellite imaging system[D]. Nanjing: Nanjing University of Science and Technology, 2009.

Atmospheric Correction of Gaofen-2 Panchromatic Satellite Images

Zheng Yang^{1,2}, Li Zhengqiang^{1,2,3*}, Wang Siheng^{4**}, Ma Yan², Li Kaitao^{1,2}, Zhang Yuhuan⁵, Liu Zhenhai⁶, Yang Leiku⁷, Hou Weizhen^{2,3}, Gu Haoran^{1,8}, Li Yinna^{2,3}, Yao Qian^{2,3}, He Zhuo^{2,3}

¹Hainan Aerospace Information Research Institute, Sanya 572032, Hainan, China;

²Aerospace Information Research Institute, State Environmental Protection Key Laboratory of Satellite Remote Sensing, Chinese Academy of Sciences, Beijing 100101, China;

³University of Chinese Academy of Sciences, Beijing 100049, China;

⁴China Academy of Space Technology, Remote Sensing Satellite General Department, Beijing 100094, China;

⁵Satellite Application Center for Ecology and Environment, MEE, Beijing 100094, China;

⁶Anhui Institute of Optics and Fine Mechanics, Hefei Institutes of Physical Science, Chinese Academy of Sciences, Hefei 230031, Anhui, China;

⁷School of Surveying and Land Information Engineering, Henan Polytechnic University, Jiaozuo 454003, Henan, China;

⁸College of Geography and Tourism, Anhui Normal University, Wuhu 241003, Anhui, China

Abstract

Objective Due to the sub-meter higher spatial resolution of panchromatic satellite images, the imaging process is easily affected by atmospheric scattering and absorption and adjacency effect under low atmospheric visibility, resulting in blurred edges of image objects and reduced image quality, and seriously affects the accuracy of quantitative remote sensing application. Before the application of panchromatic satellite image, atmospheric correction should be carried out to improve image quality. At present, the conventional atmospheric correction software can not correct the panchromatic satellite image, so the digital image processing method is often used to improve the quality of panchromatic satellite image. However, the digital image processing method often brings the problems of noise and excessive enhancement while improving the image quality. Therefore, it is urgent to develop a set of atmospheric correction methods suitable for panchromatic satellite images, eliminate the influence of atmosphere and surrounding environment on the target pixel satellite entry pupil signal, recover the real surface information, and improve image quality in the panchromatic satellite image quantitative remote sensing application.

Methods Taking the panchromatic satellite image of GF-2 as an example, this paper develops a set of atmospheric correction method for panchromatic satellite image by using the atmospheric radiative transfer model and the exponential decay point spread function. This method is simple to calculate, and fully considers the influence of atmospheric parameters (parameters of aerosol, water vapor, ozone, and other absorbing gases), spatial resolution, and adjacency effect between background pixels and target pixels on the entry pupil signal of target pixels, which further improves the image quality on the premise of ensuring the truth of panchromatic satellite image information. As an important evaluation index of an optical satellite imaging system, the modulation transfer function (MTF) can comprehensively and objectively characterize the sharpness of the image edge and the expression degree of spatial details, and its value can directly reflect the quality of imaging. Therefore, in order to comprehensively evaluate the quality of panchromatic satellite images after atmospheric correction, the traditional image quality evaluation indexes (clarity, contrast, edge energy, and detail energy) and MTF are simultaneously adopted in this paper to comprehensively and fully evaluate the atmospheric correction results.

Results and Discussions The atmospheric correction method for panchromatic satellite images developed in this paper is used to correct the GF-2 panchromatic satellite images of Baotou calibration site under two atmosphere conditions: clean atmosphere and polluted atmosphere. The results show that whether the atmospheric conditions are polluted or clean, the visual effect of the corrected panchromatic satellite images has been improved, the contours of ground objects become clear, the texture information is more abundant, and the recognition of ground objects has also been significantly improved. For high resolution panchromatic satellite images, the atmospheric correction method ignoring the adjacency effect can only improve the image brightness, but does not improve image clarity much. Especially in the case of air pollution, the edge of ground objects in the corrected image is still relatively fuzzy, which is not conducive to the visual interpretation of the image and the extraction of ground objects contour. This further proves that adjacency effect correction is essential for high resolution panchromatic satellite images. By comparing the quality evaluation parameters of each image before and after correction, it can be seen intuitively that the clarity increases by at least 155%, the contrast

increases by at least 115%, the edge energy increases by at least 247%, the detail energy increases by at least 204%, and MTF increases by at least 169%.

Conclusions Based on the 6SV radiative transfer model, the atmospheric correction method developed in this paper combines the atmospheric point spread function based on the exponential decay model, and fully considers the influence of atmospheric parameters (parameters of aerosol, water vapor, ozone and other absorbing gases), spatial resolution, and the spatial distance between background pixels and target pixels on the adjacency effect. It can effectively remove the influence of atmosphere and surrounding environment on the satellite load entry pupil signal in the process of panchromatic satellite image imaging, recover the surface truth information in the imaging area which is covered by atmospheric influence, and fully improve the quality of panchromatic satellite image under low atmospheric visibility. After the evaluation of the corrected panchromatic satellite image quality, it is found that compared with the traditional image quality evaluation index, MTF can better reflect the improvement and promotion of the sub-meter panchromatic satellite image quality by the proximity effect correction, which highlights the indispensability of the adjacency effect correction in the atmospheric correction of the panchromatic satellite image. At the same time, the trend of MTF curve and the level of the value can reflect the spatial acuity of the image and the advantages and advantages of the image quality more comprehensively and objectively. Therefore, MTF index is recommended to be included in the image quality evaluation system when sub-meter satellite images (such as panchromatic satellite images) are evaluated.

Key words atmospheric optics; panchromatic satellite images; Gaofen-2; atmospheric correction; adjacency effect correction